

September 3, 2012

Measurement of $D^0 - \bar{D}^0$ Mixing and CP Violation at *BABAR*

GIULIA CASAROSA

Università di Pisa and INFN - Sezione di Pisa
*giulia.casarosa@pi.infn.it**(on behalf of the BABAR Collaboration)*

We report on a measurement of $D^0 - \bar{D}^0$ mixing and a search for CP violation in the $D^0 \rightarrow K^+K^-$, $\pi^+\pi^-$ and $K^\pm\pi^\mp$ channels. We use D^0 's coming from D^{*+} decays, so that the flavour of the D^0 at production is tagged by the charge of the pion that is also emitted. We also use an independent set of D^0 's coming directly from the hadronization of the charm quark, but in this case the flavour of the charmed meson is not known. We analyze events collected by the *BABAR* experiment at the PEP-II asymmetric-energy e^+e^- collider, corresponding to an integrated luminosity of 468fb^{-1} . We measure the mixing parameter value to be $y_{CP} = [0.72 \pm 0.18(\text{stat}) \pm 0.12(\text{syst})]\%$, and exclude the no-mixing hypothesis at 3.3σ significance. We find no evidence of CP violation, observing $\Delta Y = [0.09 \pm 0.26(\text{stat}) \pm 0.06(\text{syst})]\%$ which is consistent with zero.

PRESENTED AT

The 5th International Workshop on Charm Physics
Honolulu, Hawai'i, May 14–17, 2012

1 Introduction

Mixing in the charm sector is a well-established phenomenon [1, 2, 3, 4, 5, 6] although there is no single measurement that exceeds 5σ significance. Recently the LHCb [7] and CDF [8] Collaborations have reported evidence of CP violation (CPV) in the difference of the integrated CP asymmetries in the $D^0 \rightarrow K^+K^-$ and $D^0 \rightarrow \pi^+\pi^-$ channels. This result was unexpected at the current experimental precision, and it may be a manifestation of New Physics (NP), although a Standard Model (SM) explanation cannot be ruled out. These measurements have renewed the interest of the community in charm physics as a sector in which to search for NP manifestations.

Under the hypothesis of CPT conservation the two mass eigenstates (D_1 and D_2) can be written in terms of the flavor eigenstates (D^0 and \bar{D}^0) as:

$$|D_{1,2}\rangle = p|D^0\rangle \pm q|\bar{D}^0\rangle \quad \text{with} \quad |p|^2 + |q|^2 = 1. \quad (1)$$

If $CP|D^0\rangle = +|\bar{D}^0\rangle$, then in the case of no CPV , D_1 is the CP -even state and D_2 the CP -odd state. The parameters that describe $D^0 - \bar{D}^0$ oscillations are proportional to the difference of masses (m_i) and widths (Γ_i) of the mass eigenstates:

$$x \equiv \frac{m_1 - m_2}{\Gamma} \quad \text{and} \quad y \equiv \frac{\Gamma_1 - \Gamma_2}{2\Gamma}, \quad (2)$$

where $\Gamma = (\Gamma_1 + \Gamma_2)/2$ is the average width. Mixing will occur if the mass eigenstates differ from the flavour eigenstates, that is, if either x or y is non-zero. SM predictions for the mixing parameter values are at the order of a percent or less and, at present, experimental measurements are in agreement with these predictions. Unfortunately the theoretical predictions are affected by large computational uncertainties on the dominant long-range-diagram contributions, preventing these measurements from being strong tests of the SM.

In the following we present a measurement of the mixing parameter y_{CP} [9] and the CP -violating parameter ΔY , defined as:

$$y_{CP} \equiv \frac{\Gamma^+ + \bar{\Gamma}^+}{\Gamma} - 1 \quad \text{and} \quad \Delta Y \equiv \frac{\Gamma^+ - \bar{\Gamma}^+}{2\Gamma}, \quad (3)$$

where Γ^+ ($\bar{\Gamma}^+$) is the average width of the D^0 (\bar{D}^0) when reconstructed in CP -even eigenstates.

The measured values of y_{CP} and ΔY constrain the parameters that govern mixing and CPV in the charm sector. Neglecting the effect of direct CP violation, estimated to be at least one order of magnitude below our current sensitivity, we relate y_{CP} and ΔY to the mixing and CP -violating parameters as follows:

$$y_{CP} = y \cos \phi - \frac{A_M}{2} x \sin \phi \quad \text{and} \quad \Delta Y = -x \sin \phi + \frac{A_M}{2} y \cos \phi. \quad (4)$$

The asymmetry $A_M = \frac{(q/p)^2 - (p/q)^2}{(q/p)^2 + (p/q)^2}$ measures CP violation in mixing, while ϕ is sensitive to CPV in the interference between decays with and without mixing, being the weak phase of the quantity $\lambda_f = \frac{q}{p} \frac{\bar{A}_f}{A_f}$ with A_f (\bar{A}_f) the amplitude for the decay D^0 (\bar{D}^0) $\rightarrow f$. In principle, ϕ can depend also on the final state, but with our current level of precision we are not sensitive to this [10]. In the absence of CP violation $y_{CP} = y$ and $\Delta Y = 0$.

2 Data Sample and Backgrounds

We reconstruct the D^0 in the h^+h^- ($h = K, \pi$) and $K^\pm\pi^\mp$ final states and measure three lifetimes:

- τ^+ for the $D^0 \rightarrow h^+h^-$ decays,
- $\bar{\tau}^+$ for the $\bar{D}^0 \rightarrow h^+h^-$ decays,
- $\tau_{K\pi}$ for the D^0 (and \bar{D}^0) $\rightarrow K^\pm\pi^\mp$ decays (the Cabibbo favored $K^-\pi^+$ and the doubly Cabibbo suppressed $K^+\pi^-$ decays are collected in the same sample).

Due to the small mixing rate ($\leq 1\%$) we can neglect the effect of mixing and assume that all signal proper time distributions are exponential. The untagged $D^0 \rightarrow K^+K^-$ sample [11] is assumed to contain 50% of D^0 and 50% of \bar{D}^0 decays. The three values of inverse lifetime are used to compute y_{CP} and ΔY : $\tau_{K\pi}$ is used to access the average width Γ while, τ^+ ($\bar{\tau}^+$) is used to obtain Γ^+ ($\bar{\Gamma}^+$).

We use *tagged* decays of the D^0 coming from D^{*+} decays, through $D^{*+} \rightarrow D^0\pi_s^+$, as well as *untagged* decays coming directly from the hadronization of the charm quark. The tagged and untagged samples are independent, *i.e.* an event containing a tagged candidate and at least one untagged candidate is excluded from the untagged sample. In the tagged sample the flavour of the D^0 is determined by the charge of the pion that is also emitted. Due to the significantly higher level of background in the $\pi^+\pi^-$ final state, we do not use the related untagged sample.

We analyze 468 fb^{-1} of data recorded by the *BABAR* detector [12] at, and slightly below, the $\Upsilon(4S)$ resonance at the e^+e^- asymmetric-energy PEP-II *B*-Factory. To avoid potential bias, we finalize our data selection criteria, as well as the procedures for fitting, extracting statistical limits, and determining systematic uncertainties, prior to examining the results.

An oppositely charged pair of K^+ or π^+ candidates satisfying particle identification criteria is fit to a common vertex to form a D^0 candidate. We require each D^0 to have momentum in the center-of-mass (CM) frame $p_{\text{CM}} > 2.5\text{ GeV}/c$ in order to remove almost completely D^0 's coming from *B*-meson decays. For the tagged modes, we form the D^{*+} candidate by fitting a D^0 candidate and a charged pion track π_s^+

to a common vertex, which is required to lie within the e^+e^- interaction region. The π_s^+ momentum is required to be greater than 0.1 GeV/ c in the laboratory frame and less than 0.45 GeV/ c in the CM frame. We veto any π_s^+ candidate that may have originated from a reconstructed photon conversion or π^0 Dalitz decay and reject a positron that fakes a π_s^+ candidate by using energy loss information. We also select tagged candidates in a Δm window, $0.1447 < \Delta m < 0.1463$ GeV/ c^2 , where Δm is the difference between the reconstructed D^{*+} and D^0 masses. This requirement strongly suppresses backgrounds.

The proper time t and proper time error σ_t of each D^0 candidate are determined from a combined fit to the D^0 production and decay vertices. The χ^2 probability of the vertex fit must satisfy $P(\chi^2) > 0.1\%$. We retain only candidates with $-2 < t < 4$ ps and $\sigma_t < 0.5$ ps. For tagged decays, this fit does not incorporate any π_s^+ information in order to ensure that the lifetime resolution models for tagged and untagged signal decays are very similar. The most probable value of σ_t for signal events is $\sim 40\%$ of the nominal D^0 lifetime [14].

For cases where multiple D^{*+} candidates in an event share one or more tracks and the D^0 decays to the same final state ($K^- \pi^+$ and $K^+ \pi^-$ are considered to be the same final state in this context), we retain only the candidate with the highest $P(\chi^2)$. If an event contains a tagged decay, all untagged candidates from that event are excluded from the final sample. In an event with no D^{*+} candidate and multiple D^0 candidates decaying to the same final state, we retain only the D^0 candidate with the highest $P(\chi^2)$. The fraction of events with multiple D^0 candidates with overlapping daughter tracks is $\ll 1\%$ for all final states.

In Fig. 1 we show the reconstructed invariant mass distributions for the selected D^0 candidates in both tagged and untagged modes. We fit the mass distributions in order to extract the total number of background candidates. In Fig. 1 we also report the fit results and, below each plot, show the normalized Poisson pulls [13]. For the tagged CP-even modes, the D^0 and \bar{D}^0 samples are fit simultaneously, sharing all parameters except for the expected signal and background candidate yields.

We perform a mode-dependent, data-driven optimization of the invariant mass window position and width, in order to reduce significantly the effects of the linear correlation between the reconstructed mass and the reconstructed proper time. The signal regions obtained for each mode are shown in Fig. 1 with dashed lines. These are 34 MeV/ c^2 wide for all modes except untagged $D^0 \rightarrow K^+ K^-$. In this mode the signal region width is reduced to 24 MeV/ c^2 due to the higher level of background, as observed in the corresponding plot. We define a lower- and a higher-mass sideband each of width 20 MeV/ c^2 ; these are used to study and characterize the combinatorial background. The mass sidebands for the untagged modes are ± 44.5 MeV/ c^2 from the signal region center. In case of the tagged modes, the distance of the sidebands from the signal region center is ± 35.5 MeV/ c^2 , and the Δm window is shifted to higher values, $0.151 < \Delta m < 0.159$ GeV/ c^2 . In the sidebands the tagged and untagged

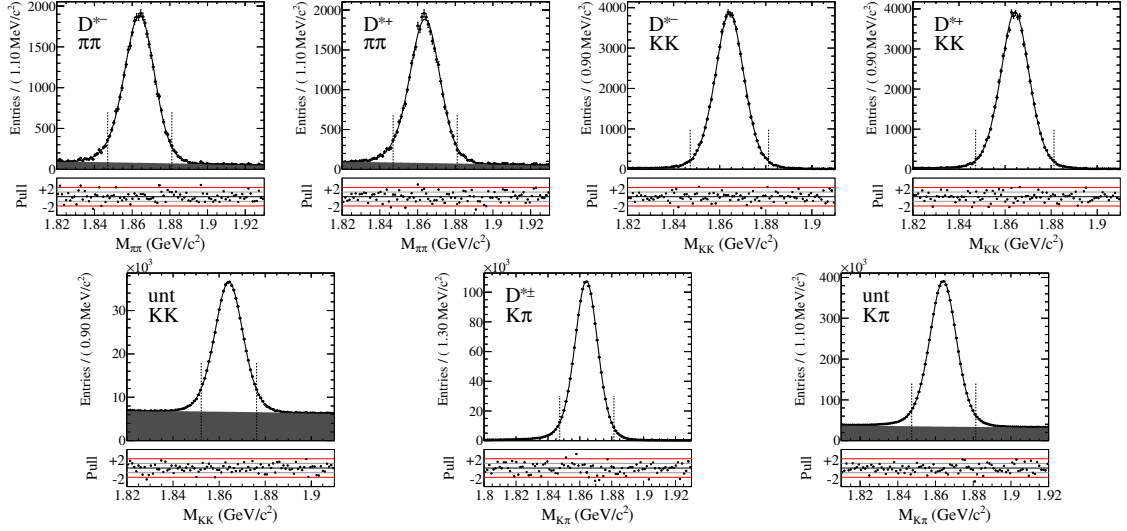


Figure 1: The reconstructed two-body mass distribution for the seven modes. The vertical lines show the *signal region*. The shaded regions are the background contributions. The normalized Poisson residuals for each fit are shown under each plot.

samples are not independent.

After the selection we divide the backgrounds into two categories. Candidates for which the common ancestor of the D^0 products is a long-living charmed meson are collected in the misreconstructed-charm background category. In Table 1 we report the composition of this background in the signal region, obtained by studying simulated events. The other background candidates, consisting mainly of random tracks, fall into the combinatorial background category. In Table 2 we report the number of signal and background candidates after selection, for the signal region.

3 Lifetime Fit

In order to extract the three lifetime values we perform an extended unbinned-maximum-likelihood fit to the 2-dimensional distribution of proper time and proper time error. All modes are fit simultaneously: the signal resolution function parameters are shared among the modes, while the background Probability Density Function (PDF) parameters are not.

The single-mode PDF for the signal events consists of an exponential convolved with a resolution function. The latter is the sum of three Gaussian functions with a common mean (offset) and widths proportional to the per-event proper time error, scaled with three different factors (one for each Gaussian). In order to take into account differences in the reconstruction due to the different final states, we multiply

Mode	Tagged Modes			Untagged Modes	
	$\pi^+\pi^-$	K^+K^-	$K^\pm\pi^\mp$	K^+K^-	$K^\pm\pi^\mp$
$D^0 \rightarrow X\ell\nu$	15.4	10.3	29.9	7.2	≤ 2
$D^0 \rightarrow K^-\pi^+$	80.8	14.9	57.1	8.8	35.8
$D^0 \rightarrow \pi^0\pi^+K^-$	1.1	70.3	1.7	63.3	6.9
$D^+ \rightarrow \pi^+\pi^+K^-$	≤ 1	2.9	≤ 1	11.8	≤ 2
$D^0 \rightarrow K^+K^-$	≤ 1	≤ 1	1.3	≤ 1	3.5
$D^0 \rightarrow \pi^+\pi^-$	1.8	≤ 1	2.2	≤ 1	3.1
$D^0 \rightarrow \pi^+\pi^-\pi^0$	≤ 1	≤ 1	7.0	≤ 1	17.3
Λ decays	≤ 1	≤ 1	≤ 1	4.9	2.6

Table 1: Expected composition of the misreconstructed-charm backgrounds. Only misreconstructed-charm background modes that have $> 1\%$ contribution in at least one signal mode are listed. For the tagged modes, the fractions are the sum of the separate D^0 and \bar{D}^0 tags.

	Signal	Combinatorial Bkgd.	Charm Bkgd.
Tagged $\pi^+\pi^-$	$65\,430 \pm 260$	3 760	97
Tagged K^+K^-	$136\,870 \pm 370$	653	309
Tagged $K^\pm\pi^\mp$	$1\,487\,000 \pm 1\,200$	2 849	642
Untagged K^+K^-	$496\,200 \pm 1\,200$	$165\,000 \pm 1\,000$	5 477
Untagged $K^\pm\pi^\mp$	$5\,825\,300 \pm 2\,600$	1 044 552	4 645

Table 2: Signal and background yields in the signal region; yields with uncertainties are those obtained directly from the lifetime fit to data. For the tagged modes, the yields are the sum of the separate D^0 and \bar{D}^0 tags.

each Gaussian scale factor by another scale factor that depends on the final state (the $K^\pm\pi^\mp$ factor is fixed to 1). In the same way we introduce a third scale factor that depends whether the mode is tagged or untagged, fixing to unity the one for the untagged modes. For the tagged CP -even modes we also take into account the wrongly-tagged signal candidates, fixing the fraction of these events to the value 0.2%, obtained from the simulated events. Since the proper time PDF depends on the proper time error, we multiply each signal PDF by the 1-dimensional binned distribution of σ_t to avoid biases. The normalization of the proper time PDF is computed for each σ_t . The σ_t histogram for the signal events is obtained from the distribution of the events in the signal region after subtraction of the misreconstructed-charm and combinatorial-background contributions.

The 2-dimensional PDF for the misreconstructed-charm background is a signal-like PDF, fitted to the simulated events and then fixed in the final fit. Since this is a physical background, its lifetime, composition and number of events change with the

mass window. Therefore we have decided not to use the sidebands to characterize it.

The combinatorial PDF is determined as a weighted average of the PDFs in the two mass sidebands, which consist of 2-dimensional histograms. For the untagged K^+K^- mode the sideband PDFs for this category are signal-like. Contributions of signal and misreconstructed-charm in the sidebands are parameterized using the simulated events, and then fixed. The weighting parameter is determined from simulated events and then is varied as part of the systematic studies.

The expected total-background candidate yields are evaluated from the mass fit and then corrected using the simulated-event information. The misreconstructed-charm contribution is estimated from the simulated events, and the combinatorial one is obtained by subtraction. In the final fit the background yields of the two categories are fixed for all modes except for the combinatorial untagged K^+K^- mode, where it is allowed to float. This became necessary since the prediction of the mass fit was not accurate enough for this mode, where the combinatorial background represents almost 25% of the events in the signal region.

4 Analysis Validation and Systematics

The validation of the procedure has been performed on four independent samples of simulated events, each equivalent to data integrated luminosity, and also on a large ensemble of pure Toy MC samples. We have also performed a qualitative validation on data by running the fit in different configurations. For example, we have fitted the tagged and untagged samples separately, finding the K^+K^- and $K^\pm\pi^\mp$ tagged and untagged extracted lifetimes compatible within the statistical uncertainties. We let the $\pi^+\pi^-$ and K^+K^- samples have different lifetimes, allowing for physical effects depending on the final states (direct CPV and the dependence of ϕ on the final state), and found τ^+ and $\bar{\tau}^+$ to be compatible for the two modes.

In addition to these tests, we have also identified sources of systematic error and have evaluated their contributions, as reported in Table 3. We have evaluated the systematic effects due to the choice of the signal region by varying its position and width. We have varied the fraction of mistagged events in the $D^0 \rightarrow h^+h^-$ tagged modes, and the fraction of D^0 's in the untagged K^+K^- mode. The proper time error PDF is obtained by subtraction of the background distributions. However, in the untagged K^+K^- mode, the combinatorial yields are extracted from the lifetime fit and not known *a priori*. In the nominal fit we first estimate the number of combinatorial events as for the other modes, and use this to perform a first simultaneous fit. We then repeat the fit using the yields just extracted, and this fit yields the nominal results. In order to evaluate the systematic error associated with this procedure we repeat the fit a third time, and take as a systematic error estimate the difference from the nominal value. We have varied the misreconstructed-charm lifetimes and yields,

Fit Variation	$ \Delta[y_{CP}] $ (%)	$ \Delta[\Delta Y] $ (%)
mass window width	0.057	0.022
mass window position	0.005	0.001
untagged KK signal σ_t PDF	0.022	0.000
mistag fraction	0.000	0.000
untagged KK D^0 fraction	0.001	0.000
charm bkgd. yields	0.016	0.000
charm bkgd. lifetimes	0.042	0.001
comb. yields	0.043	0.002
comb. sideband weights	0.004	0.001
comb. PDF shape	0.066	0.000
σ_t selection	0.052	0.053
candidate selection	0.028	0.011
Total	0.124	0.058

Table 3: The y_{CP} and ΔY systematic uncertainty estimates. The total is the sum-in-quadrature of the entries in each column.

estimated using the simulated events, by $\gtrsim 2\sigma$.

The combinatorial PDF is extracted from the sidebands after fixing the signal and misreconstructed-charm contributions. We have applied the variations described above for the misreconstructed-charm events in the signal region also in the sidebands, for both the signal and the charm-background contributions, and re-extracted the combinatorial PDF. We have also varied the number of combinatorial-background events in the signal region for the modes in which it was fixed, and the weighting parameter for each mode.

We have varied the selection criteria, in particular that on σ_t by ± 0.1 ps. We have also estimated the systematic impact of the best candidate selection by removing or keeping all the overlapping candidates. We have estimated the effects of SVT misalignment and have found these to be negligible.

5 Results and Conclusions

The seven projections of the lifetime fit are reported in Fig. 2. The following lifetime values are extracted:

$$\tau^+ = (405.69 \pm 1.25) \text{ fs}, \quad \bar{\tau}^+ = (406.40 \pm 1.25) \text{ fs}, \quad \tau_{K\pi} = (408.97 \pm 0.24) \text{ fs}. \quad (5)$$

The lifetimes are reported with the statistical error only. The $K^\pm \pi^\mp$ lifetime is compatible within one standard deviation with the PDG D^0 lifetime [14] and the

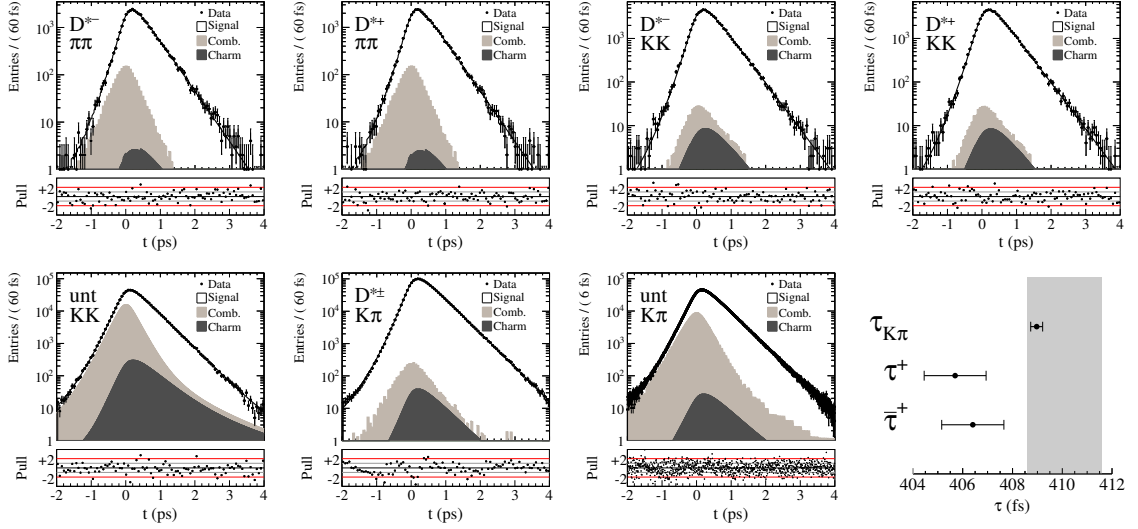


Figure 2: Proper time, t , distribution in each final state with the fit result overlaid. The combinatorial distribution (indicated as ‘Comb.’ in light gray) is stacked on top of the misreconstructed-charm distribution (indicated as ‘Charm’ in dark gray). The normalized Poisson pulls for each fit are shown under each plot; “unt” indicates the untagged datasets. The bottom-right plot shows the individual lifetime values (statistical uncertainty only); the gray band indicates the PDG D^0 lifetime $\pm 1\sigma$ [14].

CP-even lifetimes are significantly lower, as shown in the bottom-right plot of Fig. 2. Combining the values of inverse lifetime following Eq. (3), we obtain:

$$y_{CP} = (0.72 \pm 0.18 \pm 0.12)\%, \quad \text{and} \quad \Delta Y = (0.09 \pm 0.26 \pm 0.09) \text{ fs}. \quad (6)$$

The first error is statistical, obtained from the covariance matrix resulting from the fit, and the second error is systematic. This measurement represents the most precise measurement of y_{CP} , and excludes the no-mixing hypothesis at 3.3σ significance. The value of y_{CP} presented here is compatible with all previous measurements. In particular it is compatible with the previous *BABAR* measurement [3] with a probability of $\gtrsim 2\%$, taking into account that $\sim 40\%$ of the events in the current sample are also present in the samples used in the previous measurements [2, 3], and that the systematic errors are fully correlated. This result favors a lower value for y_{CP} , and approaches the value of the mixing parameter y when measured directly [15], as expected if CP is conserved. We find no evidence of CPV .

In conclusion, we report evidence of $D^0 - \bar{D}^0$ mixing with 3.3σ significance, obtaining the mixing parameter value $y_{CP} = [0.72 \pm 0.18(\text{stat}) \pm 0.12(\text{syst})]\%$. We find no evidence of CP violation, and measure the CP -violating parameter value $\Delta Y = [0.09 \pm 0.26(\text{stat}) \pm 0.06(\text{syst})]\%$.

ACKNOWLEDGEMENTS

We are grateful for the excellent luminosity and machine conditions provided by our PEP-II colleagues, and for the substantial dedicated effort from the computing organizations that support *BABAR*. The collaborating institutions wish to thank SLAC for its support and kind hospitality. This work is supported by DOE and NSF (USA), NSERC (Canada), CEA and CNRS-IN2P3 (France), BMBF and DFG (Germany), INFN (Italy), FOM (The Netherlands), NFR (Norway), MES (Russia), MICINN (Spain), STFC (United Kingdom). Individuals have received support from the Marie Curie EIF (European Union) and the A. P. Sloan Foundation (USA).

References

- [1] B. Aubert *et al.* (*BABAR* Collaboration), Phys. Rev. Lett. **98**, 211802 (2007).
- [2] B. Aubert *et al.* (*BABAR* Collaboration), Phys. Rev. D **78**, 011105 (2008).
- [3] B. Aubert *et al.* (*BABAR* Collaboration), Phys. Rev. D **80**, 071103 (2009).
- [4] M. Staric *et al.* (Belle Collaboration), Phys. Rev. Lett. **98**, 211803 (2007).
- [5] K. Abe *et al.* (Belle Collaboration), Phys. Rev. Lett. **99**, 131803 (2007).
- [6] T. Aaltonen *et al.* (CDF Collaboration), Phys. Rev. Lett. **100**, 121802 (2008).
- [7] R. Aaij *et al.* (LHCb Collaboration), Phys. Rev. Lett. **108**, 111602 (2012).
- [8] T. Aaltonen *et al.* [CDF Collaboration], arXiv:1207.2158 [hep-ex].
- [9] T. -h. (T.)Liu, In *Batavia 1994, The future of high-sensitivity charm experiments* 375-394 [hep-ph/9408330].
- [10] A. L. Kagan and M. D. Sokoloff, Phys. Rev. D **80**, 076008 (2009)
- [11] Charge conjugation is implied throughout.
- [12] B. Aubert *et al.* (*BABAR* Collaboration), Nucl. Instrum. Meth. A **479**, 1 (2002).
- [13] S. Baker and R. D. Cousins, Nucl. Instrum. Meth. **221**, 437 (1984).
- [14] K. Nakamura *et al.* (Particle Data Group), J. Phys. G **37**, 075021 (2010).
- [15] D. Asner *et al.* (HFAG Collaboration), arXiv:1010.1589 [hep-ex].